Lab on a Chip

Accepted Manuscript

ROYAL SOCIETY OF CHEMISTRY

www.rsc.org/loc

Lab on a Chip

RSCPublishing

TECHNICAL INNOVATION

Ultrasonic welding for fast bonding of self-aligned structures in lab-on-a-chip systems

Cite this: DOI: 10.1039/x0xx00000x

K. Kistrup,[a] C.E. Poulsen,[a] M.F. Hansen[a] and A. Wolff[a]

Received 00th January 2012,
Accepted 00th January 2012

DOI: 10.1039/x0xx00000x

www.rsc.org/

Ultrasonic welding is a rapid, promising bonding method for the bonding of polymer chips; yet its use is still limited. We present two lab-on-a-chip applications where ultrasonic welding can be preferably applied: (1) Self-aligned gapless bonding of a two-part chip with a tolerance of 50 μm; (2) bonding of a large area shallow chamber (1.8 cm^2 × 150 μm). Using injection moulding combined with ultrasonic welding we achieved a total production and bonding time of 60 s per chip, and a batch of chips could be produced within a day going from design to finished chips. We believe that the technical solutions offered here can significantly help bridge the gap between academia and industry, where the differences in production methods and materials pose a challenge when transferring technology.

Introduction

In the industry, ultrasonic welding is one of the leading fusion processes for thermoplastics and is ubiquitously used, historically moving from commodities, to the automotive industry, to medical devices[1,2]. Ultrasonic welding has had great impact on the plastics industry, because it is fast (rapid welding process, no curing or solvent that needs to dry), requires no soldering materials and is easy to automate. Moreover, it can be used for a range of applications, including welding of wires in electronics, embedding metal objects in plastics and fusion of virtually any thermoplastic with some cross-material compatibility[1]. A general rule of thumb is that materials of similar molecular structures and melting temperatures are compatible[3–6].

As noted by Tsao *et al.*[5], thermoplastics are well suited for microfluidic systems. However, bonding remains a critical and non-trivial step. The use of ultrasonic welding within the lab-on-a-chip research field is very limited[7–12], perhaps, because the technique is thought to have a low depth resolution and requires special chip designs with energy directors to enable reproducible ultrasonic welding[5,13]. We believe that ultrasonic welding will be a key technology, also in the lab-on-a-chip field for the following reasons: (1) it is rapid and well suited for all-polymer rapid prototyping, (2) it generates high-strength hermetic bonds, (3) the ultrasonic energy is focused on the contact points between the parts allowing the energy director to penetrate thin films[14] or membranes[11], and it prevents heating and destruction of pre-loaded reagents[15]. Moreover, combining ultrasonic welding with other mass production techniques such as injection moulding or embossing in the research phase on a lab-on-a-chip system substantially eases the transfer to commercial production of chip systems. An additional advantage is that a large number of truly single use chips can be made available in the research phase while maintaining a short time from design to prototype.

In this work, we show that ultrasonic welding can efficiently be applied to microfluidic systems and that energy directors can easily be incorporated in prototypes with parts fabricated using injection moulding[14,16]. Specifically, we demonstrate two novel aspects, where ultrasonic welding can be taken advantage of in microfluidic systems: (1) self-aligned gapless bonding of a two-part chip, and (2) sealing of low aspect ratio, large area chambers.

Ultrasonic welding of polymer chips

Ultrasonic welding is a simple thermal fusion process, where two parts are melted together by inducing vibrational friction heating at their interface. Using energy director structures the welding is localized to predefined areas of the part. Fig. 1a and b show two types of energy directors that both rely on an apex to focus the applied energy. Briefly, an ultrasonic welding machine consists of five core components: (1) a kHz range power supply, (2) a piezoelectric transducer that converts the signal to mechanical vibrations, (3) a booster horn that helps amplify and shape the vibrations, (4) a welding horn

a Department of Micro- and Nanotechnology, Technical University of Denmark, DTU Nanotech, Building 345 East, DK-2800 Kongens Lyngby, Denmark.

† Electronic Supplementary Information (ESI) available: Additional micrographs of ultrasonic welded parts and droplet PCR protocol. See DOI: 10.1039/b000000x/

(sonotrode) that provides pressure and a contact point to pass the vibrations onto the parts to be fused, (5) a fixture that prevent the parts from moving during welding. The most important parameters influencing the process are: polymer type, transducer amplitude, welding pressure and welding time/energy. Welding time is typically less than 1 second, and production rates of 20 to 60 parts per minute are routinely achievable[1].

Fabrication of polymer chips

Three chip designs (Design A1, A2, and B) are presented in this work. They are all disc shaped (⌀ = 50 mm), fitted with 12 Luer-Slip connectors[17], and are made by fusing an injection moulded main part (featuring the fluidic system) with a foil part.

Designs A1 and A2 were designed for magnetic bead-based solid phase extraction of biological targets using immiscible phase filtration as described in ref. [16]. They have the general design shown in Fig. 1c where a critical capillary microvalve structure is highlighted. Designs A1 and A2 differ by having different capillary microvalve dimensions (width = 500 and 700 µm, respectively) and by their energy director design and bonding process. Design A1 was fused via a butt joint to a flat 152 µm thick extruded foil by ultrasonic welding, see Fig. 1a. Design A2 was fused via a tongue-and-groove joint to a custom 530 µm thick injection moulded foil, see Fig. 1b. Prior to welding, the chip parts were put together manually by visual alignment of the tongue-and-groove structures and by applying a small pressure until the two parts "clicked" together.

Design B was designed for imaging, incubation and thermal cycling of droplets and is shown in Fig. 2a. It features a critical large (15 mm × 11.8 mm × 0.15 mm) chamber. It was fused via a butt joint to the 152 µm thick extruded foil.

Custom mould inserts for the injection moulder were CNC micro machined from Al sheets (grade 2017, MetalCentret, Denmark). The milling process took approx. 3-5 hours per mould insert, depending on the complexity of the design. Dimensions of the tongue-and-groove joint of Design A2 are illustrated in Fig. S1 in the supplementary Information.

All the main chip parts and the foil for Design A2 were injection moulded in cyclic olefin copolymer (COC, TOPAS 5013L-10) as described in ref. [14] with a cycle time of 40-50 s/part. The 152 µm thick extruded COC foil was of grade TOPAS 5013S-04.

Ultrasonic welding was manually performed on a Telsonic USP4700 20 kHz ultrasonic welder (Telsonic, Erlangen, Germany). The chips were mounted in a custom fixture with the foil placed on top. Design A1 was welded using a 850 N trigger force with a 0.35 s hold time. 85 J was deposited during the welding running at 80% vibrational amplitude. Design A2/B settings differed at the following parameters: Trigger force = 515/500 N; Energy = 40/60 J; Amplitude = 55/100%, respectively. The average welding time per chip was 30 s including mounting of chip and foil. Once the processes were optimised, the yield of the entire process was higher than 95%. Most failures pertained to the welding process where cracking of the foils occurred due to resonances in the chip.

The bonding strength was assessed by applying pressurised air to Design A1 and A2. Design A1 failed at 3.5 bar where the 152 µm thick foil burst, see Fig. S2 in the Supplementary Information. Design A2 remained intact after exposure to 8.5 bar, which was the highest pressure available for testing.

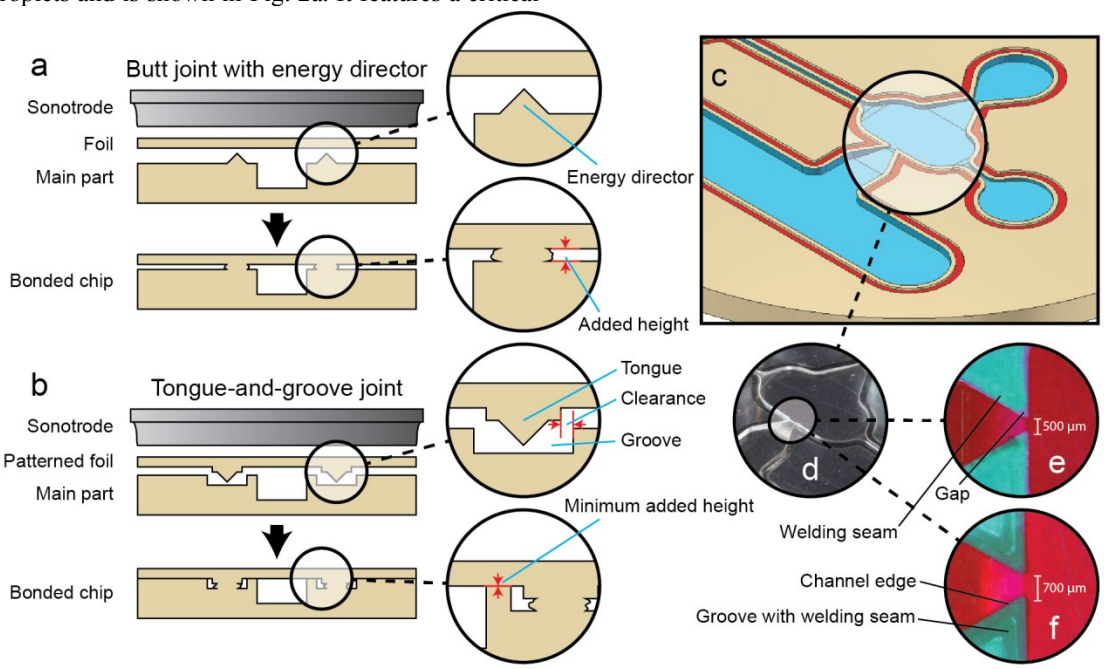

Fig. 1 Sketches of two joint types for ultrasonic welding and presentation of chip systems with like joints. (a) Sketch of butt joint energy director pre and post welding. The energy director material results in an added channel height. (b) Sketch of a tongue-and-groove joint pre and post welding. The energy director material is contained within the groove resulting in no added height. (c) Sketch of the microfluidic main part of Design A2 showing the channel system (blue) and the groove (red). (d) Photograph of ultrasonically welded chip with the same channel system featuring a butt joint. The width of the capillary microvalve is 500 µm. Parts (e) and

(f) show micrographs of Design A1 and A2 capillary microvalves, respectively, filled with a 1.3 % (V/V) sarkosyl Rhodamine B fluorescent dye solution. For the butt joint, the liquid extends outside the channel because of the added height between the chip and foil (panel (e)), whereas no liquid is observed outside the channel for the tongue-and-groove joint (panel (f)). Contrast and colour was adjusted for clarity. The darker tint of turquoise is a welding phenomenon known as flash that changes the refractive properties of the polymer. Supporting micrographs are provided in the Supplementary Information Fig. S3.

Design A: Gapless ultrasonic welding with possibility for self-aligning using energy directors

Two joint types are presented to highlight the versatility of ultrasonic welding.

Design A1 features a simple butt joint, which is the most common joint type (illustrated in Fig. 1a (schematic) and Fig. 1e (a post-welding photograph)). Butt joints are simple to integrate and require only a peripheral pattern of small energy directors to be included in the chip main part design (Fig. 1b). Moreover, no alignment is needed. However, the material from the molten energy director inevitably results in an added height to the channel. We have previously published systems featuring this type of energy director[14,16].

Design A2 features a tongue-and-groove joint. Such joints are common for macroscale objects but have until now not been implemented on microscale in lab-on-a-chip systems. Here, the energy director is situated on the foil (the tongue) and a matching peripheral groove is introduced on the chip main part, see Fig. 1b (schematic) and Fig. 1c (schematic with groove in red). The tongue-and-groove joint makes it possible to self-align the foil to the chip main part by "clicking" the two parts together prior to welding. This allows for inclusion of other features requiring alignment such as local coatings, spotted biomaterial or reagents, electrodes, and channel structures. The groove clearance of 50 µm sets the alignment tolerance of Design A2. The added channel height is eliminated, because the groove underneath the tongue contains the molten polymer from the energy director (Fig. 1b). Tongue-and-groove joints limit the choice of foils, since they have to be custom designed with appropriate structural features. However, these can be fabricated with embossing/moulding techniques, such as injection moulding, as is the case in this work.

To illustrate the performance difference of the two joint types, Designs A1 and A2 were filled with a 1.3 (V/V)% detergent (N-Lauroylsarcosine, #L7414, Sigma-Aldrich, MO, USA) containing Rhodamine B (#R6626, Sigma-Aldrich, MO, USA) solution and micrographs were taken using a Leica ZMFL III microscope. Detergent was added to ensure filling of the device, since COC is hydrophobic. Fig. 1e shows the solution flowing into the small gap of Design A1 resulting from the added height of the butt joint. In contrast, the welding seam of Design A2 perfectly follows the edge of the channel because, in addition to the welding at the tongue-and-groove welding seam, the foil and channel edge are in contact and have fused together (Fig. 1f). To further characterise the added height, the chips were investigated using a confocal microscope, see Supplementary Information Fig. S3 for details. For Design A1, an added height of 15 µm was found. Depending on the tolerance of the microfluidic system and its application, this added height can modify the behaviour compared to a system with no added height and may compromise the function of the system. No added height was detectable for Design A2.

Design B: Bonding of large area, low aspect ratio chambers

Large area, low aspect ratio (height/width) chambers have numerous uses, e.g., for cell culturing and parallelised droplet interrogation by wide field imaging[18]. Because ultrasonic welding relies on localised forces and energy deposition, it is useful for sealing large area shallow chambers, i.e., chambers with low aspect ratio geometries. Such chambers are not easily bonded thermally due to the risk of collapse of the chamber and special precautions have to be taken, for example, by selectively applying bonding pressure using a custom made bonding tool[19]. Moreover, since no new materials, such as glues or adhesives, are introduced, the temperature working range of the microfluidic system is not limited by differences in thermal expansion. To demonstrate these capabilities in a microfluidic setting, we present an all-polymer ultrasonic welded microfluidic chip featuring a single 15 mm × 11.8 mm × 0.15 mm chamber for Droplet Digital™ PCR (ddPCR), see Fig. 2a. The chamber allows for droplet packing into a single monolayer, imaged by fluorescence microscopy (Fig. 2b).

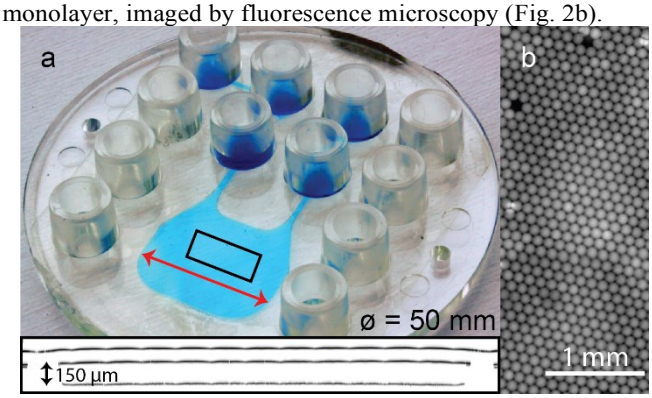

Fig. 2 (a) photograph of an ultrasonic welded polymer chip with a large area, low aspect ratio chamber for ddPCR. Inset: chamber cross section (red arrow) imaged using confocal microscopy. The three lines (top to bottom) show the outer foil surface, the inner foil surface (broken where welding has occurred), and the chip main part surface. The black double arrow denotes the channel height of 150 µm. (b) Fluorescence image of droplets for size statistics and PCR read-out.

Using a single chip, 13438 droplets were simultaneously analysed, and a target concentration of 7.2 fM was determined with 28% underestimation. More details on this application of ultrasonic welding are found in the Supplementary Information.

Discussion and conclusion

Bonding is still a recurring challenge and unsolved issue in microfluidics, where most systems are based on two or more parts that need to be fused together or interfaced with other

components. This work encourages the use of ultrasonic welding for bonding of lab-on-a-chip systems, where applicable. Ultrasonic welding provides a strong fusion with foils over a range of thicknesses (at least 100 µm – 2 mm, data not shown) and needs no special pre-treatment. It is also devoid of chemicals that may interfere with the chip application or change chip properties over time. As demonstrated in this paper, tongue-and-groove joints add a simple alignment step to the fusion process. In addition ultrasonic welding can be utilized for bonding of large area shallow chambers, expanding on the applications of ultrasonic welding within microfluidics.

In spite of these advantages, ultrasonic welding has not yet gained wide academic popularity, which may be ascribed to the fact that energy directors are required and ultrasonic welding is not compatible with thermosetting polymers such as polydimethylsiloxane (PDMS). From an industrial viewpoint, thermosetting polymers are far less attractive than thermoplastics, and it is recommended that prototypes are designed with manufacturability kept in mind for the easy implementation of larger scale testing and for future potential commercial production[23,24]. Most research in the field of microfluidics is, after all, application driven, and commercialization is often highlighted as the objective.

The chip fabrication process described here is rapid and allows for fast design iterations using commercially relevant fabrication techniques. It is possible to go from design to a 'bag of chips' within a day for Designs A1 and B; 3-5 hours micro machining, 1-2 hours injection moulding, and 1-2 hours of back-end ultrasonic welding can easily yield up to 50 ready-to-use chips. For Design A2 a second milling and injection moulding step must be included.

The bonding strength of Design A1 and A2 was assessed by applying air pressure to the chips. Design A2 was able to withstand pressures up to 8.5 bar (maximum tested), whereas Design A1 burst at 3.5 bar. As can be seen in Fig. S2 the mode of failure pertained to the bursting of the 152 µm thick foil over the channel and not the welding seam, which remained intact. This correlates well with the observation of no failure for the 500 µm thick foil of Design A2.

Design A2 has a clearance of 50 µm, see Fig. 1b and Fig. S1, which limits the alignment precision. We remark that an alignment precision of 50 µm may be sufficient for most microfluidic applications and note that no optimization was performed to minimize the clearance. If needed, this clearance can likely be further reduced.

Acknowledgements

The authors of this work would like to acknowledge Professor Dang Duong Bang for supplying PCR reagents and template DNA for the ddPCR and Marco Matteucci for help with injection moulding.

This work is funded by the Danish Council for Strategic Research through the Strategic Research Centre PolyNano (Grant no. 10-092322/DSF) and The Danish Council for Independent Research (Grant no. 09066477).

References

1. J. Rotheiser, *Joining of plastics*, 2004.
2. R. S. Soloff and S. G. Linsley, 1965, 1–6.
3. M. J. Troughton, in *Handbook of Plastics Joining - A Practical Guide*, William Andrew Publishing, Boston, 2nd edn., 2009, pp. 15–35.
4. A. Weber, *Assembly*, 2007.
5. C.-W. Tsao and D. L. DeVoe, *Microfluid. Nanofluidics*, 2008, **6**, 1–16.
6. C. Ageorges, L. Ye, and M. Hou, *Compos. Part A Appl. Sci. Manuf.*, 2001, **32**, 839–857.
7. R. Truckenmüller, Y. Cheng, R. Ahrens, H. Bahrs, G. Fischer, and J. Lehmann, *Microsyst. Technol.*, 2006, **12**, 1027–1029.
8. R. Truckenmüller, R. Ahrens, Y. Cheng, G. Fischer, and V. Saile, *Sensors Actuators A Phys.*, 2006, **132**, 385–392.
9. Y. Luo, Z. Zhang, X. Wang, and Y. Zheng, *Microelectron. Eng.*, 2010, **87**, 2429–2436.
10. Z. Zhang, Y. Luo, X. Wang, S. He, F. Meng, and L. Wang, *Microsyst. Technol.*, 2010, **16**, 2043–2048.
11. M. Bu, I. R. Perch-Nielsen, Y. Sun, and A. Wolff, in *2011 16th International Solid-State Sensors, Actuators and Microsystems Conference*, IEEE, 2011, pp. 1244–1247.
12. K. G. Lee, S. Shin, B. Il Kim, N. H. Bae, M.-K. Lee, S. J. Lee, and T. J. Lee, *Lab Chip*, 2015.
13. H. Becker and C. Gärtner, *Anal. Bioanal. Chem.*, 2008, **390**, 89–111.
14. K. Kistrup, C. E. Poulsen, P. F. Østergaard, K. B. Haugshøj, R. Taboryski, A. Wolff, and M. F. Hansen, *J. Micromechanics Microengineering*, 2014, **24**, 125007.
15. Y. Sun, J. Høgberg, T. Christine, L. Florian, L. G. Monsalve, S. Rodriguez, C. Cao, A. Wolff, J. M. Ruano-Lopez, and D. D. Bang, *Lab Chip*, 2013, **13**, 1509–14.
16. K. Kistrup, K. Skotte Sørensen, A. Wolff, and M. Fougt Hansen, *J. Magn. Magn. Mater.*, 2014, **100**, 1–6.
17. K. Ø. Andresen, M. Hansen, M. Matschuk, S. T. Jepsen, H. S. Sørensen, P. Utko, D. Selmeczi, T. S. Hansen, N. B. Larsen, N. Rozlosnik, and R. Taboryski, *J. Micromechanics Microengineering*, 2010, **20**, 055010.
18. A. C. Hatch, J. S. Fisher, A. R. Tovar, A. T. Hsieh, R. Lin, S. L. Pentoney, D. L. Yang, and A. P. Lee, *Lab Chip*, 2011, **11**, 3838–45.
19. D. S. Kim, H. S. Lee, J. Han, S. H. Lee, C. H. Ahn, and T. H. Kwon, *Microsyst. Technol.*, 2007, **14**, 179–184.
20. M. M. Kiss, L. Ortoleva-Donnelly, N. R. Beer, J. Warner, C. G. Bailey, B. W. Colston, J. M. Rothberg, D. R. Link, and J. H. Leamon, *Anal. Chem.*, 2008, **80**, 8975–81.
21. L. Mazutis, A. F. Araghi, O. J. Miller, J.-C. Baret, L. Frenz, A. Janoshazi, V. Taly, B. J. Miller, J. B. Hutchison, D. Link, A. D. Griffiths, and M. Ryckelynck, *Anal. Chem.*, 2009, **81**, 4813–21.
22. G. Jenkins, H. Zhang, Y. Zou, X. Leng, W. Zhang, and C. Yang, *rsc.org*, 2011, 945–947.
23. E. K. Sackmann, A. L. Fulton, and D. J. Beebe, *Nature*, 2014, **507**, 181–189.
24. H. Becker, *Lab Chip*, 2010, **10**, 271–3.